

Article

Kinetics and Mechanism of NO Reacting with Various Oxidation States of Myoglobin

Sara Goldstein, Gabor Merenyi, and Amram Samuni

J. Am. Chem. Soc., **2004**, 126 (48), 15694-15701 • DOI: 10.1021/ja046186+ • Publication Date (Web): 11 November 2004

Downloaded from <http://pubs.acs.org> on April 5, 2009

More About This Article

Additional resources and features associated with this article are available within the HTML version:

- Supporting Information
- Access to high resolution figures
- Links to articles and content related to this article
- Copyright permission to reproduce figures and/or text from this article

[View the Full Text HTML](#)



ACS Publications
High quality. High impact.

Kinetics and Mechanism of $\cdot\text{NO}_2$ Reacting with Various Oxidation States of Myoglobin

Sara Goldstein,^{*,†} Gabor Merenyi,[§] and Amram Samuni[‡]

Contribution from the Department of Physical Chemistry, The Hebrew University of Jerusalem, Jerusalem 91904, Department of Molecular Biology, The Hebrew University of Jerusalem—Hadassah Medical School, Jerusalem 91120, Israel, and Department of Chemistry, Nuclear Chemistry, The Royal Institute of Technology, S-10044 Stockholm 70, Sweden

Received June 28, 2004; E-mail: sarag@vms.huji.ac.il

Abstract: Nitrogen dioxide ($\cdot\text{NO}_2$) participates in a variety of biological reactions. Of great interest are the reactions of $\cdot\text{NO}_2$ with oxymyoglobin and oxyhemoglobin, which are the predominant heme proteins in biological systems. Although these reactions occur rapidly during the nitrite-catalyzed autoxidation of heme proteins, their roles in systems producing $\cdot\text{NO}_2$ in the presence of these heme proteins have been greatly underestimated. In the present study, we employed pulse radiolysis to study directly the kinetics and mechanism of the reaction of oxymyoglobin ($\text{MbFe}^{\text{II}}\text{O}_2$) with $\cdot\text{NO}_2$. The rate constant of this reaction was determined to be $(4.5 \pm 0.3) \times 10^7 \text{ M}^{-1}\text{s}^{-1}$, and is among the highest rate constants measured for $\cdot\text{NO}_2$ with any biomolecule at pH 7.4. The interconversion among the various oxidation states of myoglobin that is prompted by nitrogen oxide species is remarkable. The reaction of $\text{MbFe}^{\text{II}}\text{O}_2$ with $\cdot\text{NO}_2$ forms $\text{MbFe}^{\text{III}}\text{OONO}_2$, which undergoes rapid heterolysis along the O–O bond to yield $\text{MbFe}^{\text{V}}=\text{O}$ and NO_3^- . The perferryl-myoglobin ($\text{MbFe}^{\text{V}}=\text{O}$) transforms rapidly into the ferryl species that has a radical site on the globin ($\cdot\text{MbFe}^{\text{IV}}=\text{O}$). The latter oxidizes another oxymyoglobin ($10^4 \text{ M}^{-1}\text{s}^{-1} < k_{17} < 10^7 \text{ M}^{-1}\text{s}^{-1}$) and generates equal amounts of ferrylmyoglobin and metmyoglobin. At much longer times, the ferrylmyoglobin disappears through a relatively slow comproportionation with oxymyoglobin ($k_{18} = 21.3 \pm 5.3 \text{ M}^{-1}\text{s}^{-1}$). Eventually, each $\cdot\text{NO}_2$ radical converts three oxymyoglobin molecules into metmyoglobin. The same intermediate, namely $\text{MbFe}^{\text{III}}\text{OONO}_2$, is also formed via the reaction peroxynitrate ($\text{O}_2\text{NOO}^-/\text{O}_2\text{NOOH}$) with metmyoglobin ($k_{19} = (4.6 \pm 0.3) \times 10^4 \text{ M}^{-1}\text{s}^{-1}$). The reaction of $\cdot\text{NO}_2$ with ferrylmyoglobin ($k_{20} = (1.2 \pm 0.2) \times 10^7 \text{ M}^{-1}\text{s}^{-1}$) yields $\text{MbFe}^{\text{III}}\text{ONO}_2$, which in turn dissociates ($k_{21} = 190 \pm 20 \text{ s}^{-1}$) into metmyoglobin and NO_3^- . This rate constant was found to be the same as that measured for the decay of the intermediate formed in the reaction of $\text{MbFe}^{\text{II}}\text{O}_2$ with $\cdot\text{NO}$, which suggests that $\text{MbFe}^{\text{III}}\text{ONO}_2$ is the intermediate observed in both processes. This conclusion is supported by thermokinetic arguments. The present results suggest that heme proteins may detoxify $\cdot\text{NO}_2$ and thus preempt deleterious processes, such as nitration of proteins. Such a possibility is substantiated by the observation that the reactions of $\cdot\text{NO}_2$ with the various oxidation states of myoglobin lead to the formation of metmyoglobin, which, though not functional in the gas transport, is nevertheless nontoxic at physiological pH.

Introduction

Nitrogen dioxide ($\cdot\text{NO}_2$) participates in a variety of biological reactions. It is formed through the decomposition of peroxynitrite in the absence and presence of CO_2 ,^{1,2} during autoxidation of $\cdot\text{NO}$,^{3–5} oxidation of nitrite by heme proteins,^{6–16} and in the

reaction of peroxynitrite with metalloproteins^{15,17–21} and particularly heme proteins.^{11,22} Nitrogen dioxide is produced through

[†] Department of Physical Chemistry, The Hebrew University of Jerusalem.

[‡] Department of Molecular Biology, The Hebrew University of Jerusalem—Hadassah Medical School.

[§] Department of Chemistry, Nuclear Chemistry, The Royal Institute of Technology.

- (1) Goldstein, S.; Czapski, G. *J. Am. Chem. Soc.* **1998**, *120*, 3458–3463.
- (2) Merenyi, G.; Lind, J.; Goldstein, S.; Czapski, G. *J. Phys. Chem. A* **1999**, *103*, 5685–5691.
- (3) Ford, P. C.; Wink, D. A.; Stanbury, D. M. *FEBS Lett.* **1993**, *326*, 1–3.
- (4) Lewis, R. S.; Tannenbaum, S. R.; Deen, W. M. *J. Am. Chem. Soc.* **1995**, *117*, 3933–3939.
- (5) Goldstein, S.; Czapski, G. *J. Am. Chem. Soc.* **1995**, *117*, 12078–12084.
- (6) Arduini, A.; Mancinelli, G.; Radatti, G. L.; Hochstein, P.; Cadenas, E. *Arch. Biochem. Biophys.* **1992**, *294*, 398–402.
- (7) Wade, R. S.; Castro, C. E. *Chem. Res. Toxicol.* **1996**, *9*, 1382–1390.

- (8) Byun, J.; Mueller, D. M.; Fabjan, J. S.; Heinecke, J. W. *FEBS Lett.* **1999**, *455*, 243–246.
- (9) Reszka, K. J.; Matuszak, Z.; Chignell, C. F.; Dillon, J. *Free Radic. Biol. Med.* **1999**, *26*, 669–678.
- (10) Burner, U.; Furtmuller, P. G.; Kettle, A. J.; Koppenol, W. H.; Obinger, C. *J. Biol. Chem.* **2000**, *275*, 20597–20601.
- (11) Bourassa, J. L.; Ives, E. P.; Marqueling, A. L.; Shimanovich, R.; Groves, J. T. *J. Am. Chem. Soc.* **2001**, *123*, 5142–5143.
- (12) Lissi, E. *Free Radic. Biol. Med.* **1998**, *24*, 1535–1536.
- (13) Pietraforte, D.; Salzano, A. M.; Marino, G.; Minetti, M. *Amino Acids* **2003**, *25*, 341–350.
- (14) Herold, S. *Free Radic. Biol. Med.* **2004**, *36*, 565–579.
- (15) Nicolis, S.; Monzani, E.; Roncone, R.; Gianelli, L.; Casella, L. *Chem. Eur. J.* **2004**, *10*, 2281–2290.
- (16) Monzani, E.; Roncone, R.; Galliano, M.; Koppenol, W. H.; Casella, L. *Eur. J. Biochem.* **2004**, *271*, 895–906.
- (17) Lee, J. B.; Hunt, J. A.; Groves, J. T. *J. Am. Chem. Soc.* **1998**, *120*, 7493–7501.
- (18) Ferrer-Sueta, G.; Batinic-Haberle, I.; Spasojevic, I.; Fridovich, I.; Radi, R. *Chem. Res. Toxicol.* **1999**, *12*, 442–449.
- (19) Groves, J. T.; Lee, J.; Hunt, J. A.; Shimanovich, R.; Jin, N. *J. Inorg. Biochem.* **1999**, *74*, 28–28.

the reaction of nitrite with the ferryl oxidation state of proteins or porphyrins^{15,23,24} as well as through the reaction of peroxy-nitrite with the ferric oxidation state of these biomolecules^{11,17,22} and with oxyhemoglobin.²⁵

Of great interest are the reactions of $\cdot\text{NO}_2$ with hemeproteins and particularly with oxymyoglobin and oxyhemoglobin, which are the predominant hemeproteins in biological systems. Although these reactions occur rapidly during the nitrite-catalyzed autoxidation of hemeproteins,^{12,26–29} they were nevertheless underestimated in systems where these hemeproteins reacted with peroxy-nitrite in the absence and presence of CO_2 .^{25,30–32} An attempt to determine the rate constant for the reaction of $\cdot\text{NO}_2$ with oxymyoglobin by injection of $\cdot\text{NO}_2$ gas into oxymyoglobin solutions failed because of the rapid hydrolysis of $\cdot\text{NO}_2$ to yield NO_2^- and NO_3^- .⁷ Furthermore, there is no agreement on the mechanism of this reaction. Kosaka et al.^{26,27} have suggested that the reaction of oxyhemoglobin with $\cdot\text{NO}_2$ forms methemoglobin and NO_2^- , whereas others^{7,11,28,29} have proposed that the reaction forms perferryl-myoglobin and NO_3^- .

Nitration of proteins is currently a subject of great interest, since its occurrence has been detected in various pathological conditions.^{33–36} It has been demonstrated that the formation of $\cdot\text{NO}_2$ in the reaction of nitrite with the ferryl oxidation state of proteins can lead to nitration of tyrosine residues in proteins.^{11,13–15,23,25,37–39} However, if oxymyoglobin and oxyhemoglobin react rapidly with $\cdot\text{NO}_2$, they may compete with the tyrosyl radical for $\cdot\text{NO}_2$ and inhibit tyrosine nitration. Nevertheless, while they can serve as anti-nitrosative agents, they might also act as prooxidants if other toxic species are produced during the reaction of $\cdot\text{NO}_2$ with these hemeproteins.

In the present study, we employed pulse radiolysis to study directly the kinetics and mechanism of the reaction of oxymyoglobin with $\cdot\text{NO}_2$. We found that the rate constant for this reaction is among the fastest known for reactions of $\cdot\text{NO}_2$ with any biomolecule under physiological conditions. The biological implications are also discussed.

Experimental Section

Materials. All chemicals were of analytical grade and were used as received. Solutions were prepared with distilled water, which was further purified using a Milli-Q water purification system. Myoglobin from horse heart and reduced β -nicotinamide adenine dinucleotide (NADH) grade III from yeast were obtained from Sigma. The concentration of NADH was determined spectrophotometrically using $\epsilon_{340} = 6200 \text{ M}^{-1}\text{cm}^{-1}$. Catalase (2 mg/mL, about 130 000 U/mL) was obtained from Boehringer Mannheim. Isolated metmyoglobin ($\text{MbFe}^{\text{III}}\text{OH}_2$) or oxymyoglobin ($\text{MbFe}^{\text{II}}\text{O}_2$) solutions were prepared by adding excess of ferricyanide or dithionite, respectively, to commercial myoglobin, which always contains some metmyoglobin as well. These solutions were then subjected to chromatographic separation through a Sephadex G-25 column using 5–50 mM phosphate buffer (PB) as an eluent. Ferrylmyoglobin ($\text{MbFe}^{\text{IV}}=\text{O}$) was prepared by adding excess of H_2O_2 to metmyoglobin. The solution, which was stored on ice, proved stable for the duration of the experiment. Catalase was added immediately before each experiment to remove excess of H_2O_2 . Some buffered solutions for radiation experiments were saturated with N_2O (25 mM) or with a mixture of N_2O and O_2 prior to the addition of small volumes of the protein, the latter having been prepared at relatively high concentrations. Hence, under all experimental conditions the concentration of N_2O was higher than 16 mM while that of O_2 did not exceed 0.4 mM.

Spectrophotometric Determinations. Spectral properties of the oxidation states of myoglobin were monitored by recording the UV–visible absorption with 1, 2 or 10-mm optical path lengths using a Hewlett-Packard 8453 UV–vis diode array spectrophotometer. The concentration of each redox state was obtained from its absorption at neutral pH. The concentration of $\text{MbFe}^{\text{II}}\text{O}_2$ was determined spectrophotometrically at 410, 543, and 582 nm using $\epsilon = 128, 13.9, \text{ and } 14.4 \text{ mM}^{-1}\text{cm}^{-1}$, respectively.⁴⁰ The concentration of $\text{MbFe}^{\text{III}}\text{OH}_2$ was calculated from its absorption at 406 and 503 nm using $\epsilon = 188 \text{ and } 10.2 \text{ mM}^{-1}\text{cm}^{-1}$, respectively.⁴⁰ The concentration of $\text{MbFe}^{\text{IV}}=\text{O}$ was determined using $\epsilon_{421} = 111 \text{ mM}^{-1}\text{cm}^{-1}$. Finally, the H_2O_2 content was derived from its absorption at 240 nm using $\epsilon = 39.4 \text{ M}^{-1}\text{cm}^{-1}$. Since the spectra of metmyoglobin and ferrylmyoglobin are pH-dependent, the difference spectra between these two redox states at each of the pH values studied were determined in order to assay the oxidation/reduction yields. In those cases where two or three redox states were involved, we calculated the concentration of each species using the absorptions of the mixture at 500 (or 582), 602 and 630 nm and the extinction coefficients of each redox state at these wavelengths.

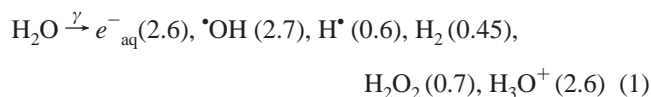
Methods. Pulse radiolysis experiments were carried out using a 5-MeV Varian 7715 linear accelerator (0.1–0.5 μs electron pulses, 200 mA current). A 200 W Xe lamp produced the analyzing light. Appropriate cutoff filters were used to minimize photochemistry. All measurements were made at room temperature using a 1-cm spectrocell and applying three light passes. The dose per pulse was determined with the Fricke dosimeter using $G(\text{Fe}^{3+}) = 1.56 \times 10^{-6} \text{ M Gy}^{-1}$ and $\epsilon_{302}(\text{Fe}^{3+}) = 2197 \text{ M}^{-1}\text{cm}^{-1}$.

Steady-state γ -irradiation was carried out at room temperature using a ^{137}Cs source with a dose rate of 9.4 Gy min^{-1} as determined by the Fricke dosimetry.

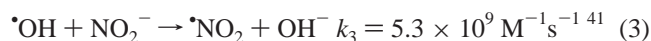
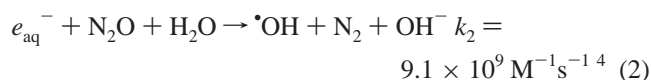
- (20) Shimanovich, R.; Hannah, S.; Lynch, V.; Gerasimchuk, N.; Mody, T. D.; Magda, D.; Sessler, J.; Groves, J. T. *J. Am. Chem. Soc.* **2001**, *123*, 3613–3614.
- (21) Ferrer-Sueta, G.; Vitturi, D.; Batinic-Haberle, I.; Fridovich, I.; Goldstein, S.; Czapski, G.; Radi, R. *J. Biol. Chem.* **2003**, *278*, 27432–27438.
- (22) Herold, S.; Shivashankar, K. *Biochemistry* **2003**, *42*, 14036–14046.
- (23) Kilinc, K.; Kilinc, A.; Wolf, R. E.; Grisham, M. B. *Biochem. Biophys. Res. Commun.* **2001**, *285*, 273–276.
- (24) Herold, S.; Rehmman, F. J. K. *Free Radic. Biol. Med.* **2003**, *34*, 531–545.
- (25) Romero, N.; Radi, R.; Linares, E.; Augusto, O.; Detweiler, C. D.; Mason, R. P.; Denicola, A. *J. Biol. Chem.* **2003**, *278*, 44049–44057.
- (26) Kosaka, H.; Imaizumi, K.; Tyuma, I. *Biochim. Biophys. Acta* **1982**, *702*, 237–241.
- (27) Kosaka, H.; Tyuma, I. *Environ. Health Perspect.* **1987**, *73*, 147–151.
- (28) Doyle, M. P.; Herman, J. G.; Duykstra, R. L. *J. Free Rad. Biol. Med.* **1988**, *1*, 145–153.
- (29) Steinhilber, R. K.; Baskin, S. I.; Clark, J. H.; Kirby, S. D. *J. Appl. Toxicol.* **1990**, *10*, 345–351.
- (30) Minetti, M.; Scorza, G.; Pietraforte, D. *Biochemistry* **1999**, *38*, 2078–2087.
- (31) Exner, M.; Herold, S. *Chem. Res. Toxicol.* **2000**, *13*, 287–293.
- (32) Herold, S.; Exner, M.; Boccini, F. *J. Am. Chem. Soc.* **2003**, *125*, 390–402.
- (33) MacMillan-Crow, L. A.; Crow, J. P.; Kerby, J. D.; Beckman, J. S.; Thompson, J. A. *Proc. Natl. Acad. Sci. USA* **1996**, *93*, 11853–11858.
- (34) Ischiropoulos, H. *Arch. Biochem. Biophys.* **1998**, *356*, 1–11.
- (35) Bachschmid, M.; Thurauf, S.; Zou, M.-H.; Ullrich, V. *FASEB J.* **2003**, *17*, 914–916.
- (36) Shishehbor, M. H.; Aviles, R. J.; Brennan, M.-L.; Fu, X.; Goormastic, M.; Pearce, G. L.; Gokce, N.; Keaney, J. F., Jr; Penn, M. S.; Sprecher, D. L.; Vita, J. A.; Hazen, S. L. *JAMA* **2003**, *289*, 1675–1680.
- (37) Brennan, M.-L.; Wu, W.; Fu, X.; Shen, Z.; Song, W.; Frost, H.; Vadseth, C.; Narine, L.; Lenkiewicz, E.; Borchers, M. T.; Lusic, A. J.; Lee, J. J.; Lee, N. A.; Abu-Soud, H. M.; Ischiropoulos, H.; Hazen, S. L. *J. Biol. Chem.* **2002**, *277*, 17415–17427.
- (38) Bian, K.; Gao, Z.; Weisbrodt, N.; Murad, F. *PNAS* **2003**, *100*, 5712–5717.
- (39) Grzelak, A.; Balcerczyk, A.; Mateja, A.; Bartosz, G. *Biochim. Biophys. Acta-Gen. Subj.* **2001**, *1528*, 97–100.

- (40) Antonini, E.; Brunori, M. *Hemoglobin and Myoglobin in Their Reactions with Ligands*; North-Holland: Amsterdam, 1971.

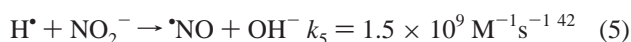
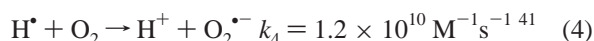
Generation of Nitrogen Dioxide. $\bullet\text{NO}_2$ was generated upon irradiation of buffered solutions containing 1 mM nitrite and saturated with a mixture of N_2O and O_2 at $\text{pH} > 7$. Under such conditions e_{aq}^- and $\bullet\text{OH}$ are converted into $\bullet\text{NO}_2$ via the following reactions



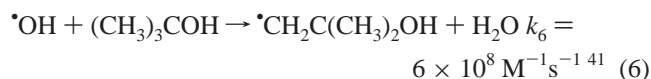
The numbers in parentheses are G-values, which represent the concentrations of the species (in $10^{-7} \text{ M Gy}^{-1}$), and are higher by about 7% in the presence of high solute concentrations.



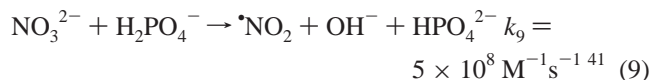
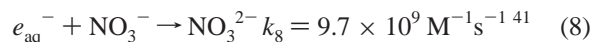
$\bullet\text{H}$ radicals are converted into $\text{O}_2^{\bullet-}$ (reaction 4) and $\bullet\text{NO}$ (reaction 5), and the corresponding yields depend on the amount of O_2 present in the solution.



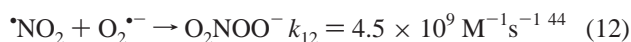
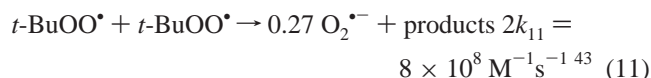
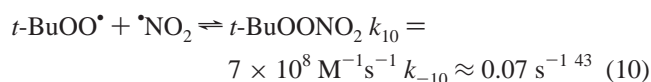
In those cases where the tested compound, such as $\text{MbFe}^{\text{II}}\text{O}_2$, reacts with nitrite, the $\bullet\text{NO}_2$ radical was formed upon irradiation of aerated solutions containing 20 mM NO_3^- , 40 mM *tert*-butyl alcohol and 12 mM PB at $\text{pH} 7.1\text{--}7.3$. Under such conditions H^\bullet is converted into $\text{O}_2^{\bullet-}$ (reaction 4), $\bullet\text{OH}$ is converted into $\bullet\text{OOCH}_2\text{C}(\text{CH}_3)_2\text{OH}$ (*t*- BuOO^\bullet) (reactions 6 and 7)



and e_{aq}^- is converted into $\bullet\text{NO}_2$ through reactions 8 and 9.



However, in systems where *tert*-butyl alcohol is used to trap $\bullet\text{OH}$ radicals, the side reactions of *t*- BuOO^\bullet (eqs 10–11) should be considered. The reaction of $\bullet\text{NO}_2$ with a tested compound has to compete with its reaction with *t*- BuOO^\bullet (reaction 10) and with $\text{O}_2^{\bullet-}$ (reaction 12), where the latter is also produced in reaction 11.



In the absence of nitrate, and when the solutions are saturated with 80% N_2O and 20% O_2 , both e_{aq}^- and $\bullet\text{OH}$ are converted into *t*- BuOO^\bullet and H^\bullet is converted into $\text{O}_2^{\bullet-}$.

Generation of Peroxynitrate ($\text{O}_2\text{NOOH}/\text{O}_2\text{NOO}^-$). Peroxynitrate was generated upon pulse irradiation of aerated solutions containing 40 mM nitrate, 0.1 M formate and 2 mM acetate buffer at $\text{pH} 4.8\text{--}5.0$ or 24 mM PB at $\text{pH} 5.9\text{--}7.2$. Under such conditions, e_{aq}^- is converted into $\bullet\text{NO}_2$ (reactions 8, 9), $\bullet\text{OH}$ and H^\bullet react with HCO_2^- to form $\text{CO}_2^{\bullet-}$, which reduces dioxygen to $\text{O}_2^{\bullet-}$, and peroxynitrate is formed via reaction 12. Consequently, $G(\text{O}_2\text{NOOH}) + G(\text{O}_2\text{NOO}^-) = G(\bullet\text{NO}_2)$, where $\text{p}K_a(\text{O}_2\text{NOOH}) = 5.9$.⁴⁵

Results and Discussion

Oxymyoglobin and metmyoglobin are inert toward NO_3^- but the former is readily oxidized by nitrite. Therefore, the reaction of $\bullet\text{NO}_2$ with $\text{MbFe}^{\text{II}}\text{O}_2$ and $\text{MbFe}^{\text{III}}\text{OH}_2$ was studied using the *tert*-butyl alcohol/ NO_3^- system by way of reduction of nitrate by e_{aq}^- as well as through the dissociation of the *t*- BuOONO_2 adduct (reaction –10). We first confirmed that neither *t*- BuOO^\bullet , nor $\text{O}_2^{\bullet-}$ nor the radiolytically produced H_2O_2 did react with $\text{MbFe}^{\text{II}}\text{O}_2$ and $\text{MbFe}^{\text{III}}\text{OH}_2$ under pulse radiolysis conditions. Indeed, no changes in the absorbance at 582 and 602 nm were observed within 40 s after pulse-irradiation of a solution, which was saturated with 80% N_2O and 20% O_2 and contained 36 μM $\text{MbFe}^{\text{II}}\text{O}_2$ or 30 μM $\text{MbFe}^{\text{III}}\text{OH}_2$, 40 mM *tert*-butyl alcohol and 12 mM PB at $\text{pH} 7.1$. In the case of $\text{MbFe}^{\text{III}}\text{OH}_2$, a slow increase of the absorption at 602 nm was observed at longer times due to a slow and progressive formation of ferrylmyoglobin in the reaction of $\text{MbFe}^{\text{III}}\text{OH}_2$ with the radiolytically produced H_2O_2 .^{46–50} Oxymyoglobin reacts much slower with H_2O_2 than $\text{MbFe}^{\text{III}}\text{OH}_2$ ⁵¹ and, therefore, its reaction with the radiolytically formed H_2O_2 could not be observed within the time scale of our pulse radiolysis experiment. Nevertheless, catalase was generally included in the reaction mixture to remove H_2O_2 .

Reaction of $\text{MbFe}^{\text{III}}\text{OH}_2$ with $\bullet\text{NO}_2$. The reaction of $\text{MbFe}^{\text{III}}\text{OH}_2$ with $\bullet\text{NO}_2$ was studied by pulse-irradiation of aerated solutions containing 30 μM $\text{MbFe}^{\text{III}}\text{OH}_2$, 20 mM NO_3^- , 40 mM *tert*-butyl alcohol and 12 mM PB at $\text{pH} 7.1$. No spectral changes were observed at 500–600 nm within 40 s after the pulse, indicating that $\bullet\text{NO}_2$ does not react with $\text{MbFe}^{\text{III}}\text{OH}_2$ under these experimental conditions. This conclusion was confirmed by steady-state irradiation of the same solution in the absence and the presence of 500 U/mL catalase. Only the appearance of the spectrum of $\text{MbFe}^{\text{IV}}=\text{O}$ was observed and this spectrum disappeared almost completely in the presence of catalase.

Reaction of $\text{MbFe}^{\text{II}}\text{O}_2$ with $\bullet\text{NO}_2$. Upon pulse-irradiation of aerated solutions containing 11–101 μM $\text{MbFe}^{\text{II}}\text{O}_2$, 20 mM NO_3^- , 40 mM *tert*-butyl alcohol and 12 mM PB at $\text{pH} 7.1$, the

- (41) Mallard, W. G.; Ross, A. B.; Helman, W. P. *NIST Standard References Database 40, Version 3.0*, 1998.
- (42) Lyman, S. V.; Schwarz, H. A.; Czapski, G. *J. Phys. Chem. A* **2002**, *106*, 7245–7250.
- (43) Goldstein, S.; Lind, J.; Merenyi, G. *J. Phys. Chem.* **2004**, *108*, 1719–1725.
- (44) Logager, T.; Sehested, K. *J. Phys. Chem.* **1993**, *97*, 10047–10052.
- (45) Goldstein, S.; Czapski, G. *Inorg. Chem.* **1997**, *36*, 4156–4162.
- (46) King, N. K.; Winfield, M. E. *J. Biol. Chem.* **1963**, *238*, 1520–1528.
- (47) Yonetani, T.; Schleyer, H. *J. Biol. Chem.* **1967**, *242*, 1974–1979.
- (48) Krishna, M. C.; Samuni, A.; Taira, J.; Goldstein, S.; Mitchell, J. B.; Russo, A. *J. Biol. Chem.* **1996**, *271*, 26018–26025.
- (49) Onuoha, A. C.; Zu, X. L.; Rusling, J. F. *J. Am. Chem. Soc.* **1997**, *119*, 3979–3986.
- (50) Giulivi, C.; Cadenas, E. *Free Radic. Biol. Med.* **1998**, *24*, 269–279.
- (51) Yusa, K.; Shikama, K. *Biochemistry* **1987**, *26*, 6684–6688.

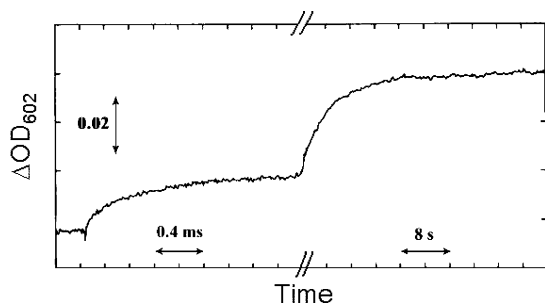


Figure 1. Reaction of $\text{MbFe}^{\text{II}}\text{O}_2$ with $\cdot\text{NO}_2$. The Absorption changes at 602 nm observed upon pulse-irradiation (11.5 Gy) of aerated solution containing 27 μM $[\text{MbFe}^{\text{II}}\text{O}_2]$, 20 mM NO_3^- , 40 mM *tert*-butyl alcohol and 12 mM PB at pH 7.1. The optical path length was 3.1 cm.

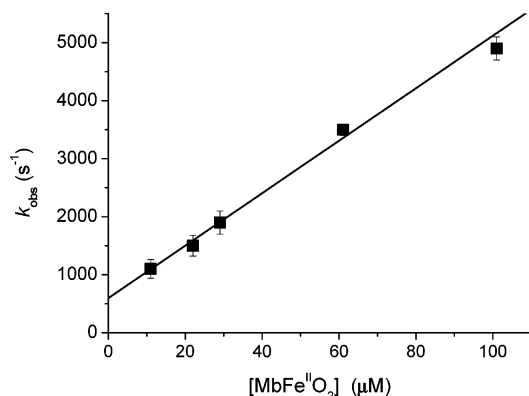


Figure 2. Concentration-dependence of $\text{MbFe}^{\text{II}}\text{O}_2$ reaction with $\cdot\text{NO}_2$. The observed first-order rate constant of the fast process as a function of $[\text{MbFe}^{\text{II}}\text{O}_2]$ as measured in aerated solutions containing 20 mM NO_3^- , 40 mM *tert*-butyl alcohol and 12 mM PB at pH 7.1 using 11.5 Gy/pulse.

absorption changes at 450–640 nm exhibited two consecutive first-order reactions, as demonstrated in Figure 1. The observed first-order rate constant of the fast process increased with increasing $[\text{MbFe}^{\text{II}}\text{O}_2]_0$ (Figure 2). The second-order rate constant, which was obtained from the slope of the line in Figure 2, is $(4.5 \pm 0.3) \times 10^7 \text{ M}^{-1}\text{s}^{-1}$. This value is considerably lower than k_{10} and k_{12} and, therefore, most $\cdot\text{NO}_2$ radicals react with *t*-BuOO \cdot forming *t*-BuOONO $_2$ rather than oxidizing $\text{MbFe}^{\text{II}}\text{O}_2$. Hence, the extent of $\text{MbFe}^{\text{II}}\text{O}_2$ oxidation observed during the fast process was relatively small. The slower first-order change of absorbance following the pulse had a rate constant $k_{\text{obs}} = 0.15 \pm 0.05 \text{ s}^{-1}$ and was independent of $[\text{MbFe}^{\text{II}}\text{O}_2]$. The major fraction of $\text{MbFe}^{\text{II}}\text{O}_2$ oxidation took place during this stage. The $\cdot\text{NO}_2$ radicals reacting during this stage originated from a relatively slow decomposition of *t*-BuOONO $_2$ to yield *t*-BuOO \cdot and $\cdot\text{NO}_2$.⁴³ During this process the steady-state concentrations of both *t*-BuOO \cdot and $\cdot\text{NO}_2$ radicals are considerably lower than that of $\text{MbFe}^{\text{II}}\text{O}_2$. This implies that $\text{MbFe}^{\text{II}}\text{O}_2$ will scavenge $\cdot\text{NO}_2$ quantitatively. Furthermore, since the rate of the reaction of $\cdot\text{NO}_2$ with $\text{MbFe}^{\text{II}}\text{O}_2$ is much larger than the rate of the reaction of $\cdot\text{NO}_2$ with *t*-BuOO \cdot , i.e., $[\text{MbFe}^{\text{II}}\text{O}_2] \gg [t\text{-BuOO}\cdot]$, the rate-determining step of the slow process is expected to be characterized by $k_{-10} \approx 0.07 \text{ s}^{-1}$.⁴³ Despite this, the observed rate constant was ca. twice as high as this value. As will be explained in more detail below, this finding is best interpreted by assuming that every homolysis through reaction –10 gives rise to the consumption of 2 molecules of $\text{MbFe}^{\text{II}}\text{O}_2$.

The difference spectra, which were monitored at the end of the fast and the slow processes, are given in Figure 3A. Comparison of the transient difference spectra recorded respec-

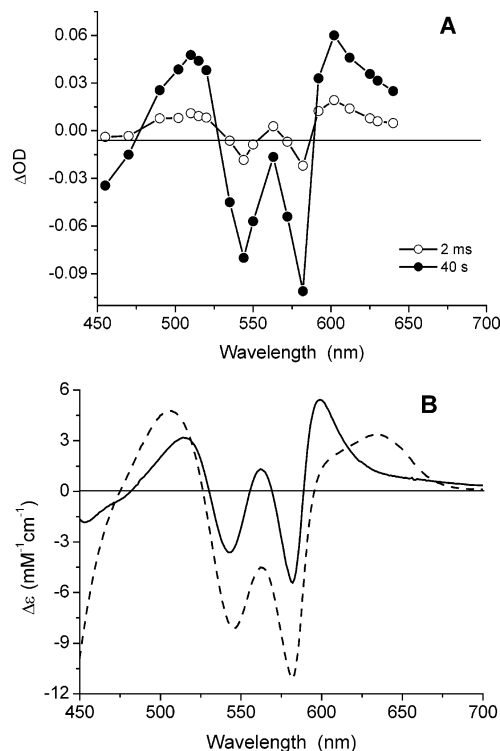


Figure 3. **A.** Transient difference spectra monitored 2 ms and 40 s after the pulse of aerated solutions containing 29 μM $\text{MbFe}^{\text{II}}\text{O}_2$, 20 mM NO_3^- , 40 mM *t*-butanol and 12 mM PB at pH 7.1 using 11.5 Gy/pulse and 3.1 cm optical path. **B.** Difference spectra at pH 7.1 between $\text{MbFe}^{\text{III}}\text{OH}_2$ and $\text{MbFe}^{\text{II}}\text{O}_2$ (dashed) and $\text{MbFe}^{\text{IV}}=\text{O}$ and $\text{MbFe}^{\text{II}}\text{O}_2$ (solid).

tively at 2 ms and 40 s after the pulse (Figure 3A) with the difference spectra between $\text{MbFe}^{\text{III}}\text{OH}_2$ and $\text{MbFe}^{\text{II}}\text{O}_2$ or $\text{MbFe}^{\text{IV}}=\text{O}$ and $\text{MbFe}^{\text{II}}\text{O}_2$ (Figure 3B) reveals that during the first 2 ms the reaction of $\text{MbFe}^{\text{II}}\text{O}_2$ with $\cdot\text{NO}_2$ forms only $\text{MbFe}^{\text{IV}}=\text{O}$. However, by 40 s after the pulse a mixture of $\text{MbFe}^{\text{IV}}=\text{O}$ and $\text{MbFe}^{\text{III}}\text{OH}_2$ is observed. This observation is further substantiated by a comparison between the ratios of the absorbance changes at specific wavelengths, such as $\Delta\text{OD}_{602}/\Delta\text{OD}_{582}$, $\Delta\text{OD}_{630}/\Delta\text{OD}_{582}$ and $\Delta\text{OD}_{602}/\Delta\text{OD}_{563}$.

To determine more accurately the yields of $\text{MbFe}^{\text{IV}}=\text{O}$ and $\text{MbFe}^{\text{III}}\text{OH}_2$ in the reaction mixture, the absorption spectrum of the irradiated solution was scanned by a diode array spectrophotometer 40 s after the pulse. Since NADH reduces $\text{MbFe}^{\text{IV}}=\text{O}$ to $\text{MbFe}^{\text{III}}\text{OH}_2$,⁴⁸ the experiment was repeated with NADH being added to the solution 40 s after pulse-irradiation. The difference spectra monitored after pulse-irradiation of 29 μM $\text{MbFe}^{\text{II}}\text{O}_2$, with or without 1 mM NADH being added after the irradiation, are presented in Figure 4. The spectra clearly demonstrate the reduction of the ferryl into the ferric state. The oxidation yield in the absence of NADH was calculated using the two isosbestic points of $\text{MbFe}^{\text{IV}}=\text{O}$ and $\text{MbFe}^{\text{III}}\text{OH}_2$ at 519 nm ($\Delta\epsilon_{519} = 3 \text{ mM}^{-1}\text{cm}^{-1}$) and 616 nm ($\Delta\epsilon_{616} = 2.6 \text{ mM}^{-1}\text{cm}^{-1}$), and was within the accuracy of the experimental measurements identical to the yield of $\text{MbFe}^{\text{III}}\text{OH}_2$ obtained upon the addition of NADH. The oxidation yield was independent of the dose and of $[\text{MbFe}^{\text{II}}\text{O}_2]_0$, when the latter varied between 29 and 94 μM . This yield was $G = 4.4 \pm 0.4$, which is about twice the yield of $\cdot\text{NO}_2$ reacting with $\text{MbFe}^{\text{II}}\text{O}_2$. Using the known spectra of the various redox states at pH 7.1, we determined the ratio of the yield of $\text{MbFe}^{\text{IV}}=\text{O}$ to that of $\text{MbFe}^{\text{III}}\text{OH}_2$ by 40 s after the pulse as 1.06 ± 0.11 .

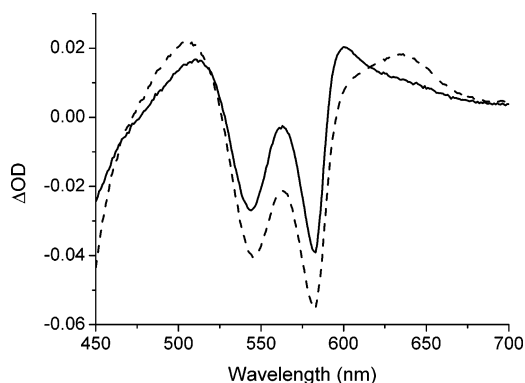
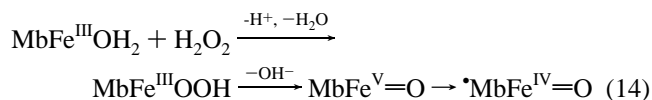


Figure 4. Transient difference spectra monitored 40 s after the pulse (solid) and upon the addition of 1 mM NADH 40 s after the pulse (dashed). The aerated solutions contained 29 μM $\text{MbFe}^{\text{II}}\text{O}_2$, 20 mM NO_3^- , 40 mM *tert*-butyl alcohol and 12 mM PB at pH 7.15. The dose was 11.5 Gy and the optical path length was 1 cm.

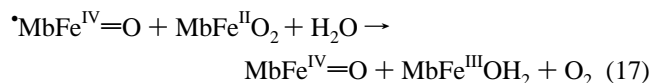
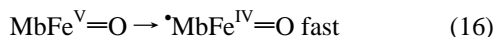
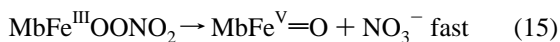
We, therefore, suggest that $\cdot\text{NO}_2$ adds to $\text{MbFe}^{\text{II}}\text{O}_2$ to form $\text{MbFe}^{\text{III}}\text{OONO}_2$ as a short-lived intermediate (reaction 13), and $k_{13} = (4.5 \pm 0.3) \times 10^7 \text{ M}^{-1}\text{s}^{-1}$ was determined from the slope of the line in Figure 2. The intercept in this plot represents mainly the competition between $\text{MbFe}^{\text{II}}\text{O}_2$ and *t*-BuOO \cdot for $\cdot\text{NO}_2$ radicals.



Chemically, $\text{MbFe}^{\text{III}}\text{OONO}_2$ is akin to the short-lived peroxy adduct, which most probably is formed as an intermediate in the reaction of $\text{MbFe}^{\text{III}}\text{OH}_2$ with H_2O_2 . It is widely believed that this adduct yields a ferryl having the radical site on the globin, $\cdot\text{MbFe}^{\text{IV}}=\text{O}$ (eq 14).^{46–50}



On the basis of this analogy, we propose that $\text{MbFe}^{\text{III}}\text{OONO}_2$ decomposes via heterolysis of the O–O bond to form $\text{MbFe}^{\text{V}}=\text{O}$ and NO_3^- (reaction 15). Subsequently, $\text{MbFe}^{\text{V}}=\text{O}$ rapidly transforms into $\cdot\text{MbFe}^{\text{IV}}=\text{O}$ (reaction 16), which oxidizes $\text{MbFe}^{\text{II}}\text{O}_2$ (reaction 17).



Hence, the redox species formed within 2 ms after the pulse should be $\cdot\text{MbFe}^{\text{IV}}=\text{O}$, which is expected to absorb similarly to $\text{MbFe}^{\text{IV}}=\text{O}$ at 450–700 nm.^{46,47} Then, within 40 s, reaction 17 produces equal amounts of $\text{MbFe}^{\text{IV}}=\text{O}$ and $\text{MbFe}^{\text{III}}\text{OH}_2$. The observed rate constant of the slow process was ca. twice as high as $k_{-10} = 0.07 \text{ s}^{-1}$ and was almost unaffected by $[\text{MbFe}^{\text{II}}\text{O}_2]_0 = 11\text{--}101 \mu\text{M}$. The simplest way of explaining this finding is to assume that, as long as $[\text{MbFe}^{\text{II}}\text{O}_2]_0 > 11 \mu\text{M}$, $k_{17}[\text{MbFe}^{\text{II}}\text{O}_2]_0 \gg k_{-10} = 0.07 \text{ s}^{-1}$. With these assumptions 2 molecules of $\text{MbFe}^{\text{II}}\text{O}_2$ will be consumed for every homolysis in reaction –10 and hence $k_{\text{obs}} = 2k_{-10}$. According to this interpretation k_{17} must be significantly higher than $0.07/10^{-5} \approx 10^4 \text{ M}^{-1}\text{s}^{-1}$. On the other hand, as no formation of $\text{MbFe}^{\text{III}}\text{OH}_2$ was observed

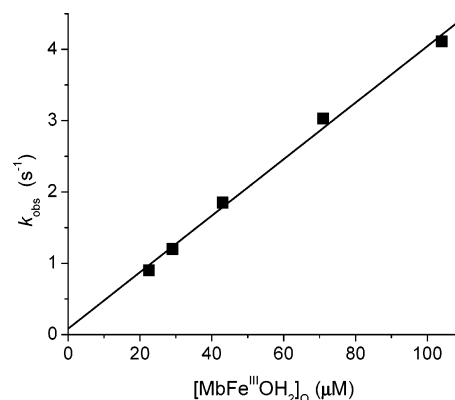
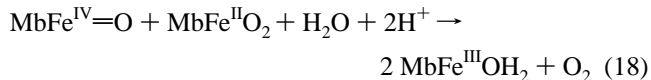


Figure 5. Concentration-dependence of $\text{MbFe}^{\text{III}}\text{OH}_2$ reaction with peroxynitrate. The observed first-order rate constant of the formation of the absorbance at 580 nm as measured upon pulse-irradiation of aerated solutions containing 40 mM NO_3^- , 0.1 M formate and 2 mM acetate buffer at pH 4.8 using 16 Gy/pulse.

during the fast process, k_{17} must be much smaller than k_{13} . In conclusion, $10^4 \text{ M}^{-1}\text{s}^{-1} < k_{17} < 10^7 \text{ M}^{-1}\text{s}^{-1}$.

The rate constant for the reaction of $\text{MbFe}^{\text{II}}\text{O}_2$ with H_2O_2 is relatively small, namely $k = 20.8 \text{ M}^{-1}\text{s}^{-1}$ ⁵¹, and considering the low concentration of the radiolytically formed H_2O_2 , this reaction can be ignored during the spectrophotometric experiments.

We note that the yield of $\text{MbFe}^{\text{III}}\text{OH}_2$ increased slowly with time at the expense of $\text{MbFe}^{\text{IV}}=\text{O}$ even in the presence of catalase. Within 1 h after the pulse it approached $G(\text{MbFe}^{\text{III}}\text{OH}_2) = 7.0$, i.e., $G(\text{MbFe}^{\text{III}}\text{OH}_2) \approx 3 G(\cdot\text{NO}_2)$. We attribute this slow process to the comproportionation of $\text{MbFe}^{\text{II}}\text{O}_2$ with $\text{MbFe}^{\text{IV}}=\text{O}$ (reaction 18).



To study reaction 18, we mixed 22 μM $\text{MbFe}^{\text{IV}}=\text{O}$ with 225 μM $\text{MbFe}^{\text{II}}\text{O}_2$ at pH 7.1. The increase in the absorption at 633 nm followed first-order kinetics resulting in $k_{\text{obs}} = (2.4 \pm 0.6) \times 10^{-3} \text{ s}^{-1}$ and $\Delta\text{OD}_\infty = 0.16 \pm 0.01$, implying $k_{18} = 21.3 \pm 5.3 \text{ M}^{-1}\text{s}^{-1}$. This value is similar to those determined for the comproportionation reactions of bovine and human oxyhemoglobin, namely 19 and 23 $\text{M}^{-1}\text{s}^{-1}$, respectively.⁵² The stoichiometry of Reaction 18 is obtained from the respective absorbance changes using $\Delta\epsilon_{633} = 3.4 \text{ mM}^{-1}\text{cm}^{-1}$ as $\Delta[\text{MbFe}^{\text{III}}\text{OH}_2]/\Delta[\text{MbFe}^{\text{IV}}=\text{O}] = 2.1 \pm 0.1$.

Reaction of $\text{MbFe}^{\text{III}}\text{OH}_2$ with Peroxynitrate. O_2NOOH is similar to HOOH in that both are relatively resistant to homolysis of the O–O bond. We, therefore, hypothesized that their reactions with $\text{MbFe}^{\text{III}}\text{OH}_2$ should also be similar. Peroxynitrate ($\text{O}_2\text{NOO}^-/\text{O}_2\text{NOOH}$, $\text{p}K_a = 5.9$)^{44,45} was produced from superoxide ($\text{HO}_2^\cdot/\text{O}_2^{\cdot-}$, $\text{p}K_a = 4.8$) and $\cdot\text{NO}_2$ by pulse irradiation of aerated solutions containing 0.1 M formate, 40 mM NO_3^- and 2 mM PB at pH 4.8–5.1 or 24 mM PB at pH 5.9–7.2. The reaction of $\text{MbFe}^{\text{III}}\text{OH}_2$ with peroxynitrate could be studied because its precursors, i.e., $\text{O}_2^{\cdot-}$ and $\cdot\text{NO}_2$, were found to react extremely slowly with $\text{MbFe}^{\text{III}}\text{OH}_2$. To study the reaction kinetics, the absorption changes at 580 nm upon pulse-irradiation of 22–105 μM $\text{MbFe}^{\text{III}}\text{OH}_2$ were followed. The rate of the build up of the absorption at 580 nm obeyed first-order kinetics, and k_{obs} was linearly dependent on $[\text{MbFe}^{\text{III}}\text{OH}_2]_0$ (Figure 5). The

(52) Giulivi, C.; Davies, K. *J. Biol. Chem.* **1990**, *265*, 19453–19460.

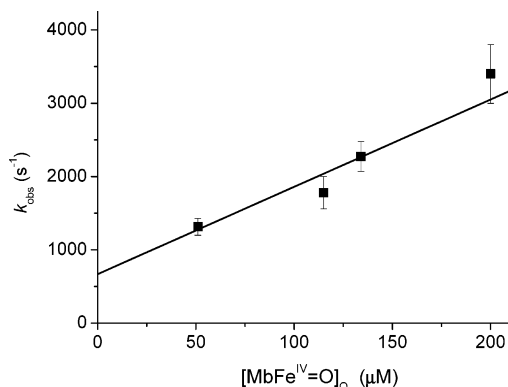
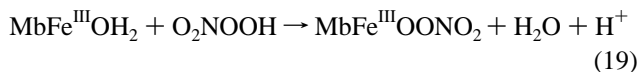


Figure 6. Concentration-dependence of MbFe^{IV}=O reaction with $\bullet\text{NO}_2$. The observed first-order rate constant of the fast process as a function of [MbFe^{IV}=O] as measured at 638 nm in N₂O/O₂ ([N₂O] > 15 mM) saturated solutions containing 1 mM NO₂⁻, and either 2 mM borate buffer at pH 9.7 or 20 mM PB at pH 10.3 using 16 Gy/pulse.

apparent bimolecular rate constant was unaffected by increasing the pH, and at pH > 6.5 the absorption yield was too small for accurate measurements. These observations demonstrate that O₂NOOH and O₂NOO⁻ react with MbFe^{III}OH₂ at similar rates. At pH > 6.5 the absorption increase was relatively small due to an efficient competition of the self-decomposition of O₂NOO⁻ ($k = 1.3 \text{ s}^{-1}$ 25 °C)^{44,45} with its reaction with MbFe^{III}OH₂.

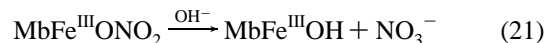
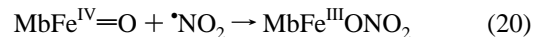
The species formed after the pulse was identified as MbFe^{IV}=O. The yield of MbFe^{IV}=O exceeded 95% of the peroxynitrate initially formed ($\Delta\epsilon_{580} = 5.4 \text{ mM}^{-1}\text{cm}^{-1}$ at pH 4.8 between the extinction coefficients of MbFe^{IV}=O and MbFe^{III}OH₂). We, therefore, suggest that MbFe^{IV}=O is formed by Reaction 19 followed by reactions 15 and 16.



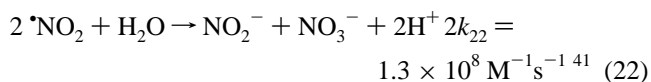
From the slope of the line in Figure 5, we obtained $k_{19} = (4.6 \pm 0.3) \times 10^4 \text{ M}^{-1}\text{s}^{-1}$. This value is close to $1.03 \times 10^4 \text{ M}^{-1}\text{s}^{-1}$ ¹¹ and $(6.6 \pm 0.3) \times 10^4 \text{ M}^{-1}\text{s}^{-1}$,²² the rate constant of MbFe^{III}OH₂ reacting with ONOOH/ONOO⁻, which are similar in size and acid base properties to O₂NOOH/O₂NOO⁻. As discussed above, MbFe^{III}OONO₂ undergoes rapid heterolysis of the O–O bond to form $\bullet\text{MbFe}^{\text{IV}}=\text{O}$ (Reactions 15–16). Even in the absence of potential reductants, such as MbFe^{II}O₂, the half-life of $\bullet\text{MbFe}^{\text{IV}}=\text{O}$ is relatively short,^{47,50,53} eventually yielding the more stable nonradical ferryl species MbFe^{IV}=O.

Reaction of MbFe^{IV}=O with $\bullet\text{NO}_2$. Since MbFe^{IV}=O was found to be stable in the presence of 1 mM nitrite at pH > 9.7 for the duration of the experiment, $\bullet\text{NO}_2$ radicals could be generated through the oxidation of nitrite by $\bullet\text{OH}$. Relatively small volumes of aerated solutions of MbFe^{IV}=O were added to N₂O-saturated solutions containing 1 mM nitrite and 2 mM borate at pH 9.7 or 20 mM PB at pH 10.3, which were pulse-irradiated within a few minutes of preparation. In these solutions the concentration of N₂O was higher than 16 mM whereas that of O₂ did not exceed 0.4 mM. A rapid first-order build-up of a transient absorption was observed at 638 nm, which decayed via a first-order reaction leaving behind a residual persistent absorption. The observed first-order rate constant of the fast formation process increased with increasing [MbFe^{IV}=O]₀

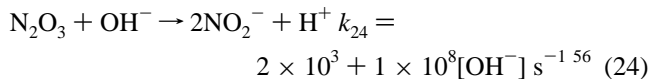
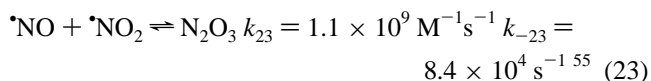
(Figure 6), whereas that of the slow decay process was independent of [MbFe^{IV}=O]₀ with $k_{\text{obs}} = 190 \pm 20 \text{ s}^{-1}$. These results were unaffected upon replacing 2 mM borate with 20 mM PB or by varying the pH from 9.7 to 10.3. In analogy with the suggestion of Herold et al.,⁵⁴ we propose that MbFe^{IV}=O is reduced by $\bullet\text{NO}_2$ via the formation of the transient species MbFe^{III}ONO₂.



Hence, $k_{21} = 190 \pm 20 \text{ s}^{-1}$ and from the slope of the line in Figure 6 we determined $k_{20} = (1.2 \pm 0.2) \times 10^7 \text{ M}^{-1}\text{s}^{-1}$. The intercept in this plot represents the competition between the reaction of $\bullet\text{NO}_2$ with MbFe^{IV}=O (reaction 20) and the dimerization/hydrolysis of $\bullet\text{NO}_2$ (reaction 22).



Reactions 20 and 21 imply a stoichiometry of [MbFe^{III}OH]/[$\bullet\text{NO}_2$] = 1. We determined the stoichiometry of this process using γ -radiolysis. Under such conditions, the dimerization/hydrolysis of $\bullet\text{NO}_2$ (reactions 22) and the reaction of $\bullet\text{NO}_2$ with $\bullet\text{NO}$ (Reactions 23 and 24), which is formed via reaction 5, can be ignored.



Upon γ -radiolysis of a solution saturated with 80% N₂O and 20% O₂ containing 43.2 μM MbFe^{IV}=O, 1.2 mM NO₂⁻, 1000 U/mL catalase and 5 mM borate buffer at pH 9.8, the yield of MbFe^{III}OH increased linearly with the dose. The difference spectra obtained following irradiation were compared to that measured for 43.2 μM MbFe^{IV}=O under the same experimental conditions. From the slope of the lines in Figure 7 we determined $G(\text{MbFe}^{\text{III}}\text{OH}) = 6.7 \pm 0.3$. This high value implies that $G(\text{MbFe}^{\text{III}}\text{OH}) \approx G_{\text{OH}} + G_{\text{e}} + G_{\text{H}}$. As the H[•] atoms in this system convert NO₂⁻ to $\bullet\text{NO}$ (Reaction 5), the measured G-value reflects the ability of $\bullet\text{NO}$ to reduce additional MbFe^{IV}=O to MbFe^{III}OH. A similar experiment performed using a solution containing 21.6 μM MbFe^{IV}=O at pH 10.25 (5.7 mM borate, 1.3 mM NO₂⁻, 1000 U/mL catalase, 88% N₂O, 12% O₂) resulted in $G(\text{MbFe}^{\text{III}}\text{OH}) = 5.9 \pm 0.2$. While still very high, this value is somewhat lower than the one obtained at higher [MbFe^{IV}=O]₀, and could be attributed to a higher scavenging efficiency of $\bullet\text{NO}_2$ and $\bullet\text{NO}$ by 43.2 μM MbFe^{IV}=O.

Herold et al.⁵⁴ studied by pulse radiolysis the reaction of MbFe^{IV}=O with $\bullet\text{NO}_2$ in N₂O-saturated solutions containing 1.5 μM MbFe^{IV}=O, 10 mM nitrite and 50 mM borate at pH 9.5. They assumed that, practically all the primary radicals formed by the pulse, produced exclusively $\bullet\text{NO}_2$ (150 μM). In

(54) Herold, S.; Exner, M.; Nauser, T. *Biochemistry* **2001**, *40*, 3385–3395.

(55) Gratzel, M.; Taniguchi, S.; Henglein, A. *Berichte Der Bunsen-Gesellschaft Fur Physikalische Chemie* **1970**, *74*, 488–492.

(56) Treinin, A.; Hayon, E. *J. Am. Chem. Soc.* **1970**, *92*, 5821–&.

(53) Gunther, M. R.; Sturgeon, B. E.; Mason, R. P. *Free Radic. Biol. Med.* **2000**, *28*, 709–719.

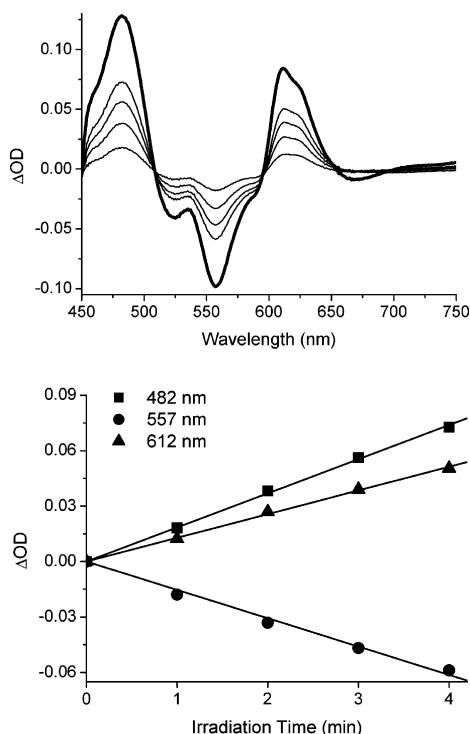


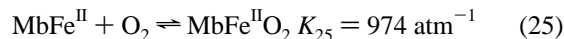
Figure 7. Reaction of MbFe^{IV}=O with •NO₂. The difference spectra obtained upon γ -irradiation of a solution saturated with 80% N₂O and 20% O₂ containing 43.2 μ M MbFe^{IV}=O, 1.2 mM NO₂⁻, 500 U/mL catalase and 5 mM borate at pH 9.8 for 1, 2, 3 and 4 min at dose rate of 9.4 Gy min⁻¹. The bold line is the difference spectrum between 43.2 μ M MbFe^{III}-OH and 43.2 μ M MbFe^{IV}=O under the same conditions. The dependence of the yield of MbFe^{III}OH on the dose resulted in G(MbFe^{III}OH) = 6.7 \pm 0.3.

this single experiment they obtained $k_{20} = 1 \times 10^7 \text{ M}^{-1}\text{s}^{-1}$, which is close to our value. However, their derived value of $k_{21} = 35 \pm 5 \text{ s}^{-1}$ is seen to be significantly lower than that determined in the present work, i.e., $k_{21} = 190 \pm 20 \text{ s}^{-1}$. We note, however, that under their experimental conditions ca. 15% of e_{aq}⁻ and all H• radicals react with NO₂⁻ to form •NO. Hence, the initial concentrations of •NO₂ and •NO should be about 140 and 26 μ M, respectively. Therefore, the hydrolysis of •NO₂ (Reaction 22) and the fast reaction of •NO with •NO₂ (Reaction 23) have to be taken into account. Under these circumstances, all •NO₂ decayed within 2 ms, and Herold et al.⁵⁴ could not have determined k_{20} by assuming pseudo-first-order conditions with [•NO₂]₀ = 150 μ M. Most importantly, due to the poorly defined radical mixture their derived value for k_{21} is bound to be seriously distorted. By contrast, given that in our measurements reaction 20 proceeds in clean pseudo-first-order conditions and reactions 20 and 21 are well-separated, the present value of $k_{21} = 190 \pm 20 \text{ s}^{-1}$ is believed to be rather accurate. In another set of experiments Herold et al.⁵⁴ reacted MbFe^{II}O₂ with •NO and observed an intermediate, which decayed with $k = 205 \pm 5 \text{ s}^{-1}$. Since this intermediate appeared to decay much faster than the one obtained in reaction 20, Herold et al.⁵⁴ argued that the former must be MbFe^{III}OONO. However, given that in the present study the two rate constants are essentially identical, we suggest that in both situations the only observable intermediate is MbFe^{III}OONO₂. We note that the intermediate that Herold et al.⁵⁴ produced in the reaction between MbFe^{II}O₂ with •NO decayed much faster at low than at high pH. In fact, this intermediate was not even seen at pH 7. Similar pH dependences were reported for the decay of other anion adducts to MbFe^{III},

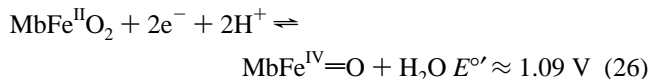
such as MbFe^{III}NO₂⁴⁰ or MbFe^{III}N₃.⁵⁷ Upon raising the pH, deprotonation at various sites occurs, which changes the overall charge of the protein. As the heterolysis of the adduct involves charge separation, this process is expected to be sensitive to the overall charge, which accounts for these observations. On the other hand, homolysis of the putative MbFe^{III}OONO intermediate would not entail charge separation. Consequently, no obvious rationalization accounts for its apparent pH-dependence. Our assignment of MbFe^{III}OONO₂ to the observable intermediate implies that MbFe^{III}OONO must undergo completely or at least to a major extent an instantaneous conversion to its isomer, MbFe^{III}OONO₂, which has a much lower free energy than MbFe^{III}OONO. This conversion is believed to be initiated by homolysis of the O–O bond to yield a geminate pair of MbFe(IV)=O + •NO₂. Between 80%¹¹ and 100%⁵⁴ of the latter collapses to the cage product MbFe^{III}OONO₂, while the rest, if any, escapes out of the solvent cage as freely diffusible MbFe(IV)=O and •NO₂.

We estimate that the O–O bond in MbFe^{III}OONO is significantly weaker than even in alkylperoxynitrites. In fact, while the homolysis of alkyl peroxynitrites is still slightly endergonic, the corresponding homolysis of MbFe^{III}OONO is almost certainly exergonic. These conclusions are borne out by the following arguments.

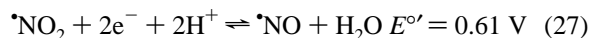
The equilibrium constant for reaction 25 at pH 7.0 and 25 °C has been determined to be 974 atm⁻¹.⁵⁸



Using reduction potentials at pH 7 vs. NHE with $E^\circ(\text{MbFe}^{\text{III}}\text{OH}_2/\text{MbFe}^{\text{II}}) \approx 0.0 \text{ V}$,⁵⁹ $E^\circ(\text{MbFe}^{\text{IV}}=\text{O}/\text{MbFe}^{\text{III}}\text{OH}_2) \approx 0.90 \text{ V}$,⁶⁰ and $E^\circ(\text{O}_2/\text{H}_2\text{O}) = 0.815 \text{ V}$,⁶¹ we calculate $E^\circ(26) \approx 1.09 \text{ V}$.



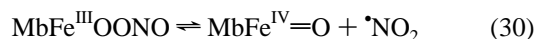
Similarly, from $\Delta G_f^\circ(\bullet\text{NO}_2, \text{aq}) = 15.1 \text{ kcal/mol}$,⁶² $\Delta G_f^\circ(\bullet\text{NO}, \text{aq}) = 24.4 \text{ kcal/mol}$ ⁶² and $\Delta G_f^\circ(\text{H}_2\text{O}, \text{l}) = -56.7 \text{ kcal/mol}$,⁶¹ we calculate $E^\circ(27) = 0.61 \text{ V}$.



Combining $E^\circ(26)$ with $E^\circ(27)$ we obtain $\Delta G^\circ \approx -22 \text{ kcal/mol}$ for the overall oxygen transfer reaction 28



Reaction 28 can be subdivided into reactions 29 and 30:



We can generalize reactions 29 and 30, where we shall treat

- (57) Lin, J.; Merryweather, J.; Vitello, L. B.; Erman, J. E. *Arch. Biochem. Biophys.* **1999**, *361*, 148–158.
 (58) Schenkman, K. A.; Marble, D. R.; Burns, D. H.; Feigl, E. O. *J. Appl. Physiol.* **1997**, *82*, 86–92.
 (59) Blankman, J. I.; Shahzad, N.; Dangi, B.; Miller, C. J.; Guiles, R. D. *Biochemistry* **2000**, *39*, 14799–14805.
 (60) He, B.; Sinclair, R.; Copeland, B. R.; Makino, R.; Powers, L. S.; Yamazaki, I. *Biochemistry* **1996**, *35*, 2413–2420.
 (61) Dean, J. A., Ed. *Lange's Handbook of Chemistry*, 13 ed.; McGraw-Hill: New York.
 (62) Stanbury, D. M. *Adv. Inorg. Chem.* **1989**, *33*, 69–138.

the cases for $X = \text{H}$, alkyl or MbFe



From published data^{43,62–64} we calculate $\Delta G^\circ(31) = -18.3$ and ca. -17.3 kcal/mol for $X = \text{H}$ and $X = \text{alkyl}$, respectively. The corresponding values for $\Delta G^\circ(32)$ come out as 14.1 and ca. 4.3 kcal/mol. We note that, upon replacing an alkyl group by MbFe, the exergonicity of the overall oxygen transfer reaction increases by 9 kcal/mol, i.e., ΔG° goes from -13 to -22 kcal/mol. Furthermore, from a comparison of H to alkyl, the homolysis reaction 32 would appear substantially more sensitive to X than reaction 31. Since in the former reaction the integrity of the O–O bond is disrupted, while in the latter it is not, this finding is not unexpected. We have no experimental data for $\Delta G^\circ(29)$ and $\Delta G^\circ(30)$. However, the rate of O–N homolysis of $\text{Cr}_{\text{aq}}\text{OONO}_2^{2+}$ into $\text{Cr}_{\text{aq}}\text{OO}^{2+}$ and $\cdot\text{NO}_2$ is reported to be faster by ca. 3 orders of magnitude, i.e., $\sim 180 \text{ M}^{-1}\text{s}^{-1}$,⁶⁵ than that for ROONO_2 into $\text{ROO}\cdot$ and $\cdot\text{NO}_2$, i.e., $\sim 0.1 \text{ M}^{-1}\text{s}^{-1}$.⁴³ This shows that the N–O bond in transition metal peroxynitrates is probably weaker than in alkyl peroxynitrates. It is reasonable to assume that the same applies for the corresponding peroxynitrites. Hence, we are confident that $\Delta G^\circ(29) > -17$ kcal/mol. Consequently, $\Delta G^\circ(30)$ should be less than -5 kcal/mol, and on this basis the homolysis reaction 30 is predicted to be significantly exergonic. Given that the lifetime of alkyl peroxynitrites is below $1 \mu\text{s}$,^{43,63} the lifetime of $\text{MbFe}^{\text{III}}\text{OONO}$ is expected to be even shorter. Hence, this intermediate should be undetectable under any experimental circumstances.

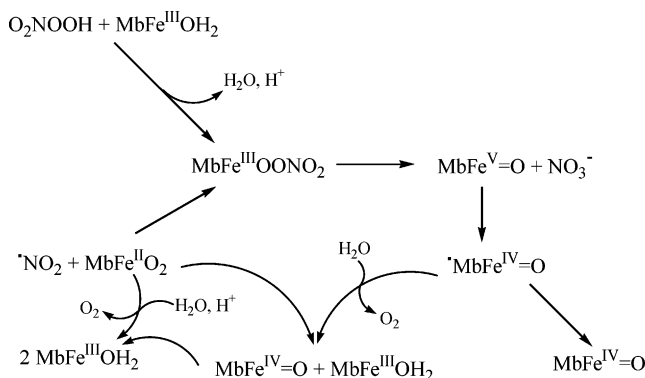
The above reasoning concerns the production of free XO and $\cdot\text{NO}_2$. However, the rate-determining step in the decay of XOONO is homolysis to yield a geminate pair. It is seen that, at a given exergonicity of reaction 32 (or 30), the smaller the yield of cage escape the larger the exergonicity of homolysis to form the geminate pair. For $X = \text{alkyl}$, the yield of cage escape is ca. 15%,^{43,63} while for $X = \text{MbFe}$ it is 0–20%.^{11,66} For the highest yield the relative exergonicities of Reaction 32 and geminate pair formation are about the same for $X = \text{alkyl}$ and $X = \text{MbFe}$. Should the escape yield for $X = \text{MbFe}$ turn out to be very small, perhaps below 1%, the exergonicity of its homolysis to form the geminate pair increases even further relative to $X = \text{alkyl}$. Thus, the conclusion about the short lifetime of MbFeOONO remains even more valid.

Finally, we note that the exergonicity of homolysis precludes the reverse reaction –30 from taking place at a significant rate. This is consistent with the exclusive formation of $\text{MbFe}^{\text{III}}\text{ONO}_2$ in reaction 20.

Conclusions

The present study focused on the stoichiometry, kinetics and mechanisms of $\cdot\text{NO}_2$ reacting with oxymyoglobin and ferrylmyoglobin. The interconversion among the various oxidation states of myoglobin that is prompted by nitrogen oxide species is remarkable (Scheme 1).

Scheme 1



The rate constant for reaction of $\cdot\text{NO}_2$ with oxymyoglobin was determined to be $k_{13} = (4.5 \pm 0.3) \times 10^7 \text{ M}^{-1}\text{s}^{-1}$, and is among the highest rate constants measured for $\cdot\text{NO}_2$ with any biomolecule, i.e., similar to those for the reaction of $\cdot\text{NO}_2$ with glutathione, cysteine, and urate at pH 7.4.⁶⁷ As proposed in Scheme 1, the reaction of $\cdot\text{NO}_2$ with oxymyoglobin forms $\text{MbFe}^{\text{III}}\text{OONO}_2$, which undergoes rapid heterolysis along the O–O bond to yield $\text{MbFe}^{\text{V}}\text{=O}$ and NO_3^- . The ferrylmyoglobin rapidly transforms into $\cdot\text{MbFe}^{\text{IV}}\text{=O}$, which oxidizes another oxymyoglobin ($10^4 \text{ M}^{-1}\text{s}^{-1} < k_{17} < 10^7 \text{ M}^{-1}\text{s}^{-1}$) and generates equal amounts of ferrylmyoglobin and metmyoglobin. Over a much longer time period, the ferrylmyoglobin disappears by way of a relatively slow comproportionation with oxymyoglobin ($k_{18} = 21.3 \pm 5.3 \text{ M}^{-1}\text{s}^{-1}$). Eventually, each $\cdot\text{NO}_2$ radical converts three oxymyoglobin molecules into metmyoglobin (Scheme 1). The same adduct, namely $\text{MbFe}^{\text{III}}\text{OONO}_2$, is formed via the reaction of metmyoglobin with O_2NOOH ($k_{19} = (4.6 \pm 0.3) \times 10^4 \text{ M}^{-1}\text{s}^{-1}$), and this reaction generates ferrylmyoglobin and nitrate (Scheme 1). The reaction of $\cdot\text{NO}_2$ with ferrylmyoglobin ($k_{20} = (1.2 \pm 0.2) \times 10^7 \text{ M}^{-1}\text{s}^{-1}$) yields $\text{MbFe}^{\text{III}}\text{ONO}_2$, which in turn dissociates ($k_{21} = 190 \pm 20 \text{ s}^{-1}$) into metmyoglobin and NO_3^- . The same intermediate is produced in the reaction of $\text{MbFe}^{\text{II}}\text{O}_2$ with $\cdot\text{NO}$.

The potential physiological implications of this chemistry are that heme proteins can be instrumental in detoxifying $\cdot\text{NO}_2$, and hence in pre-empting deleterious processes, such as nitration of proteins. This conclusion is substantiated by the observation that the reactions of $\cdot\text{NO}_2$ with the various oxidation states of myoglobin lead to the formation of metmyoglobin, which, though not functional in the gas transport, is nevertheless nontoxic at physiological pH.

Acknowledgment. This research was supported by grants from the U.S.–Israel Binational Science Foundation (No. 2002013). G.M. is grateful for the financial support given by the Swedish Science Council (VR).

Note Added after ASAP Posting. After this paper was posted ASAP on November 11, 2004, two authors' affiliations were corrected, the label for eq 21 was added, and the E° notation in the text below eq 25 was corrected. The corrected version was posted November 16, 2004.

(63) Merenyi, G.; Lind, J.; Goldstein, S. *J. Am. Chem. Soc.* **2002**, *124*, 40–48.

(64) Merenyi, G.; Lind, J.; Czapski, G.; Goldstein, S. *Inorg. Chem.* **2003**, *42*, 3796–3800.

(65) Pestovsky, O.; Bakac, A. *Inorg. Chem.* **2003**, *42*, 1744–1750.

(66) Herold, S. *Comptes Rendus Biologies* **2003**, *326*, 533–541.

JA046186+

(67) Ford, E.; Hughes, M. N.; Wardman, P. *Free Radic. Biol. Med.* **2002**, *32*, 1314–1323.